Green Chemistry

PAPER

View Article Online
View Journal | View Issue

Cite this: *Green Chem.*, 2024, **26**, 9729

Exploiting natural complexity for substrate controlled regioselectivity and stereoselectivity in tantalum catalysed hydroaminoalkylation†

Cameron H. M. Zheng, [a] Ben E. Nadeau, [a] Heather L. Trajano *[b] and Laurel L. Schafer *[a]

Received 2nd April 2024,
Accepted 6th June 2024

DOI: 10.1039/d4gc01614a

rsc.li/greenchem

Naturally occurring and structurally diverse alkene-containing substrates, terpenes, provided a platform for establishing chemo-, regio-, and diastereoselective reactivity in tantalum catalysed hydroaminoalkylation. Naturally derived 1,3-butadienes revealed the unique regio- and diastereoselective (*Z*)-1,4-addition products accessible from isoprene and β-myrcene by hydroaminoalkylation. Selective terpene functionalisation, within an industrially produced turpentine mixture, demonstrates functionalisation specificity of β-pinene and limonene. Lastly, sesquiterpene functionalisation using β-caryophyllene and humulene provide rare examples of trisubstituted alkene reactivity in hydroaminoalkylation, by leveraging strain-release and stereoelectronic effects to control chemoselectivity. As a result of these reactivity studies using natural substrates, new tools for understanding alkene electronic, strain, and stereoelectronic effects on chemo- and diastereoselectivity outcomes have revealed new mechanistic insights into hydroaminoalkylation.

Introduction

Structurally complex natural products have traditionally served as inspiring synthetic targets for chemists.[1–3] Alternatively, natural products, such as terpenes, have been extensively utilised as low-cost enantiopure starting materials for synthesis (Fig. 1).[4,5]

Terpenes themselves also have therapeutic applications ranging from antimicrobial agents to tumour suppressants.[6–8] This natural bioactivity has inspired medicinal chemists to use terpenes as templates for the synthesis of terpenoid derivatives in which medicinal properties may be enhanced.[9,10] Notably, terpenes contain reactive alkenes in their framework, and may contain other functional groups. The C–C double bonds of the alkene or their adjacent C–H bonds ($R_2C{=}CR{-}C\mathbf{H_2}{-}$) bonds may be transformed to yield functionalized synthetic terpenoid products bearing new C–C, C–Si, C–O, C–N, and C–P bonds for example.[11–20]

Amines are highly prevalent functional groups in pharmaceuticals and are featured in over 40% of drugs in the FDA's approved small molecule drug database.[21] As a result, chemists are highly motivated to develop efficient methods for amination.[22,23] Amination of terpene frameworks can result in enhanced bioactivity relative to their unfunctionalized precursors.[24] Hydroaminoalkylation is a catalytic atom economic[25] reaction which activates the α C–H bond of an amine, followed by addition across an unsaturated C–C bond (Scheme 1).[26–28] This reaction produces two possible regioisomers, branched and linear, *via* 1,2-insertion or 2,1-insertion of the alkene, respectively. This transformation is catalysed by photoredox catalysis,[29] early,[30–34] and late[35–38] transition metal catalysts. Generally, photoredox and late transition metal catalysis favour the linear product, while early transition metal catalysts favour the branched product.

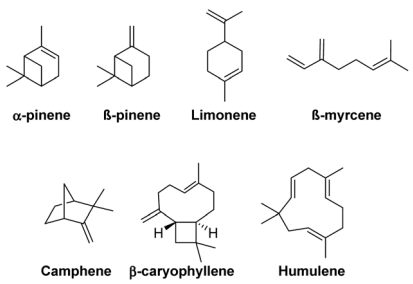

Fig. 1 Structural variability in terpene frameworks.

[a]*Department of Chemistry, University of British Columbia, Vancouver, British Columbia, V6T 1Z1, Canada. E-mail: schafer@chem.ubc.ca*
[b]*Department of Chemical and Biological Engineering, University of British Columbia, Vancouver, British Columbia, V6T 1Z3, Canada*

†Electronic supplementary information (ESI) available. CCDC 2238920 and 2344466. For ESI and crystallographic data in CIF or other electronic format see DOI: https://doi.org/10.1039/d4gc01614a

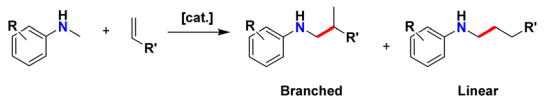

Scheme 1 General hydroaminoalkylation reaction scheme.

Our group has focused on the development of 1,3-*N*,*O*-chelated early transition metal hydroaminoalkylation catalysts using group 4 and 5 metals.[30,39–44] The inclusion of a hemilabile 1,3-*N*,*O*-chelating ligand in the design of catalysts has greatly enhanced reactivity such that reaction temperatures and times have decreased from 160 °C to room temperature and from days to minutes.[26,30,40,42] Now early transition metal hydroaminoalkylation catalysts bearing 1,3-*N*,*O*-chelates can be used with aryl, and alkyl amines,[40,44] as well as N-heterocycles,[31] for reactions with activated and unactivated, terminal and internal alkenes,[40,41,45] as well as alkynes.[39,46] Currently, *in situ* generated catalysts from **Ta(CH$_2$SiMe$_3$)$_3$Cl$_2$** with ureate ligands are the state-of-the-art catalysts for the hydroaminoalkylation of challenging unactivated alkenes with excellent selectivity for the branched product.[31,40,44,47] Further, these catalysts can be used with challenging macromolecular/polymeric substrates and under neat reaction conditions.[45,48,49] Hydroaminoalkylation, as an atom-economic transformation with no by-products, can be readily coupled in synthetic sequences to efficiently assemble complex amine products. For example, we recently reported a telescoped sequence furnishing *N*-alkyl/arylated indoles, leveraging the unique bond-disconnection enabled by hydroaminoalkylation.[50] As such, hydroaminoalkylation represents a Green Advance in the synthesis of amine and N-heterocyclic molecules and materials.

Terpenes, with their inherent structural complexity, are important renewable and abundant biomass-derived starting materials for a range of hydrofunctionalisation reactions.[14–17,19,51–56] To date, terpenes have been rarely explored in hydroaminoalkylation reactivity (Scheme 2).[47] We previously reported exquisite chemoselectivity for the geminal di-substituted alkene of limonene, over reactivity with the tri-substituted alkene, and diastereospecific reactivity with β-pinene to generate the branched product in both cases. No racemization of the existing stereocentres in either substrate was observed when using our catalyst, in contrast to late transition metal hydrofunctionalisation of terpenes.[57]

Here we expand on these results to show that a range of terpenes provide synthetic opportunities to enhance substrate scope and achieving the synthesis of varied synthetic terpenoid alkaloids. These structurally complex starting materials also provide a platform for developing mechanistic insights into chemo-, regio- and stereoselective reactivities in alkene hydroaminoalkylation. This work illustrates how the natural complexity of renewable terpene starting materials, coupled with the principles of Green Chemistry,[58] advance critical C–H functionalisation technologies for the direct amination of alkenes.

Results and discussion

Isoprene is a natural product produced by both plants and humans and is one of the most abundant non-methane volatile organic compounds in our atmosphere.[59] This abundant natural product contains a 1,3-butadiene moiety which can serve as a source of naturally-found conjugated dienes. The use of 1,3-butadiene as substrates has not been reported previously in tantalum-catalysed hydroaminoalkylation, thus we were highly motivated to test the reactivity of isoprene (Scheme 3). Based upon established reactivity trends with terminal and *gem*-disubstituted alkenes,[40,47] we anticipated the selective formation of branched product, **Branched**.

Here, 10 mol% **Ta(CH$_2$SiMe$_3$)$_3$Cl$_2$** and sodium ureate ligand (**L$^-$Na$^+$**) generated the active tantalum-ureate catalyst in toluene-d_8, for the functionalisation of isoprene with

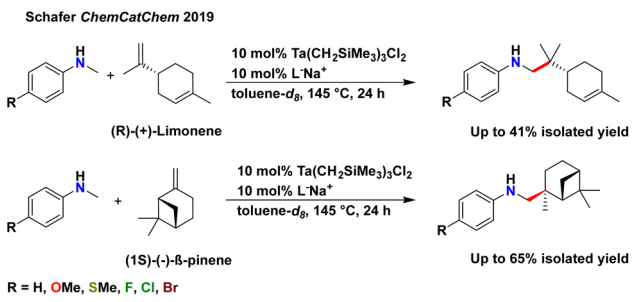

Scheme 2 Previously demonstrated limonene and β-pinene functionalisation by hydroaminoalkylation.[47]

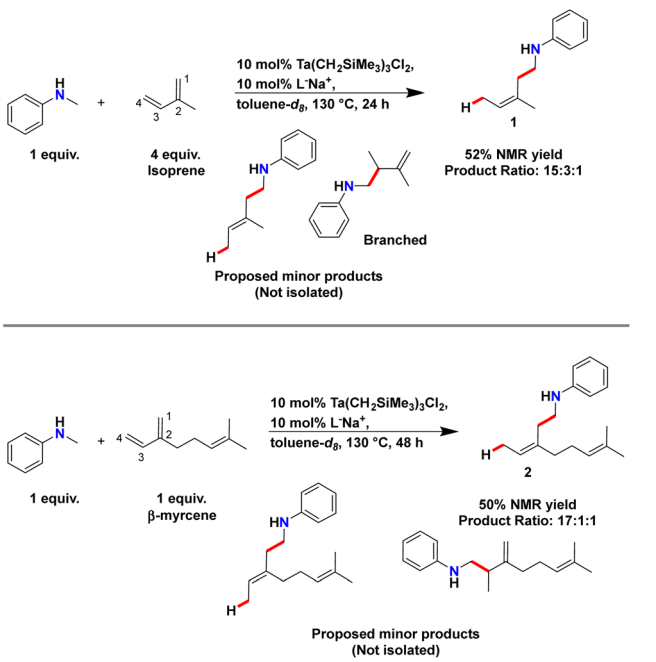

Scheme 3 Synthesis of **1** and **2** by hydroaminoalkylation. Yields were calculated by ^{1}H NMR spectroscopy using 1,3,5-trimethoxybenzene as internal standard. Product ratios were determined by GC.

N-methylaniline. *N*-Methylaniline was chosen as amine for exploratory alkene reactivity studies as it is the most reactive amine with our **Ta** catalyst. Though our tantalum-ureate catalyst is typically capable of achieving high yields using a 1 : 1 amine : alkene ratio, the volatility of isoprene (~34 °C boiling point) meant that 4 equivalents were needed to ensure substantial amounts of isoprene were not lost to evaporation during reaction set up. 1,3,5-Trimethoxybenzene (**TMB**) was used as internal standard to determine ^{1}H NMR yields. Integration of the aniline product **1** *ortho* C–H resonances at 6.44 ppm *vs.* the 6.13 ppm resonance of TMB and compared to the 6.35 ppm resonance of unreacted *N*-methylaniline allowed for *in situ* reaction monitoring. The preferred reaction conditions of Scheme 3 showed that the extra equivalents of isoprene also afforded a higher ^{1}H NMR yield of **1** (52%) *versus* the use of only 1 equivalent of isoprene (*ca.* 23%).

Surprisingly, 2D NMR spectroscopy revealed that the major product **1** resulted from 1,4-*addition* across the 1,3-butadiene to form the *Z*-diastereomer. Analysis by Gas Chromatography-Mass Spectrometry (**GC-MS**) of the reaction mixture prior to purification gave a 15 : 3 : 1 product ratio, further demonstrating high selectivity for the 1,4-regioisomer with *Z*-stereochemistry. This regioselectivity is different from our anticipated product and is different from selective 4,1-*addition* product obtained when using a zirconium tethered-bisureate catalyst system for the hydroaminoalkylation of isoprene.[60]

To determine if this regioselectivity was unique to isoprene, we extended the investigation to include the naturally-sourced monoterpene, β-myrcene. This substrate includes not only a 1,3-butadiene but a trisubstituted alkene within its structure. Like isoprene, 10 mol% of $\mathbf{Ta(CH_2SiMe_3)_3Cl_2}$ and $\mathbf{L^-Na^+}$ allowed for functionalisation of β-myrcene with *N*-methylaniline to access **2** in 50% NMR yield, where TMB served as internal standard (Scheme 3). After product isolation by silica gel chromatography, structural elucidation of major product **2** confirmed the preferred formation of the 1,4-*addition* product with *Z*-diastereoselectivity. Further analysis by GC-MS of the reaction mixture after heating revealed a product ratio of 17 : 1 : 1. Thus, early-transition metal ureate catalysts favour 1,3-diene isomerization for hydroaminoalkylation, and tantalum-ureates favour 1,4-*addition* while zirconium-ureates favour 4,1-*addition*.[60]

Reported examples of 1,3-diene hydroaminoalkylation using 1-phenyl-1,3-butadiene and titanium metal catalysts afford either a mixture of branched (3,4-*addition*, major product) and linear products (4,3-*addition*),[61,62] with the 4,1-*addition* product being observed as a minor regioisomer in one case.[33] Ruthenium hydroaminoalkylation catalysts also access 4,1-*addition* products from isoprene and hydantoins.[38] A comparable metallaphotoredox hydroaminoalkylation system featuring an iridium and cobalt catalyst pairing produced the 1,4-*addition* product as the major product (2 : 1 ratio *vs.* the 4,3-*addition* product) from isoprene and *N*,*N*-dimethylaniline in a 2 : 1 *E* : *Z* ratio.[29] With β-myrcene using the same metallaphotoredox system, the 4,1-*addition* product is favoured, rather than 1,4-*addition*, but with greater diastereoselectivity favouring the *E*-diastereomer (20 : 1 *E* : *Z* ratio). Our yields of a single product from isoprene and β-myrcene functionalisation are comparable to photoredox-based methodologies. We propose that the relatively high tantalum catalyst loadings, 10 mol%, needed to furnish **1** and **2** in ~50% yield are due to trace impurities which may be present in our natural product substrates.

Extensive mechanistic investigations into early transition metal catalysed hydroaminoalkylation, both experimental[43,63–65] and computational,[66–68] have provided key insights that inform a proposed mechanism for the highly regio- and diastereoselective 1,4-*addition* outcome observed here (Scheme 4). The observation and isolation of related zirconium π-allyl intermediates resulting from 1,3-diene hydroaminoalkylation have also informed this proposal.[60] Thus, in summary our proposed mechanism for tantalum catalysed 1,3-diene hydroaminoalkylation invokes readily isomerized tantalum π-allyl intermediates, coupled with a turnover limiting protonolysis step, to result in Curtin–Hammett control over regio- and stereoselectivity. A more detailed analysis is provided below.

For early transition metal catalysed hydroaminoalkylation of terminal alkenes, 1,2-*insertion* of alkene is preferred due to electronic effects which favour the build-up of negative charge on the primary carbon which adds α to metal position of the resultant expanded metallacycle.[68,69] As a result, we may have expected an initial 4,3-*insertion* of 2-substituted-1,3-dienes into the reactive tantallaaziridine (Scheme 4). However, the diene offers a directing group effect, thereby favouring the formation of a π-allyl intermediate, thus facilitating the 2,1-*insertion* which ultimately produces the 1,4-*addition* product regioselectivity. In related zirconium catalysed hydroaminoalkylation of 1-phenyl-1,3-dienes, diene insertion was observed to be reversible.[60] Thus, here we propose that the observed excellent regioselectivity for the 1,4-*addition* product with

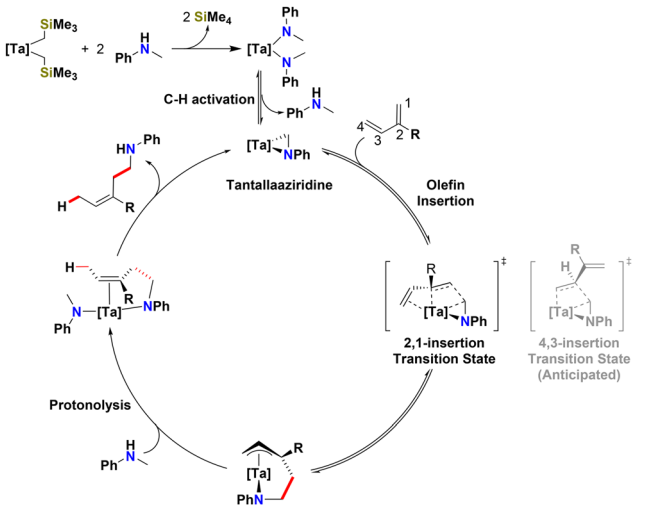

Scheme 4 Proposed catalytic cycle for the hydroaminoalkylation of 1,3-butadienes to give the 1,4-addition product with *Z*-diastereoselectivity.

Z-diastereoselectivity can be attributed to the reversible formation of π-allyl intermediates that undergo turnover limiting protonolysis later in the catalytic cycle.[69]

With regioselective chemistry established with various terpene substrates, we wanted to test the robustness of our catalyst using a raw commercial distillate, turpentine. Turpentine is a fluid distilled at 150 °C from pine tree resin,[51] particularly rich in α-pinene, β-pinene and limonene amongst other monoterpenes. Amounts of each of the terpene components can vary depending on tree species and its geographical location, or by the extraction method.[51] Turpentine has been used throughout history as medicine, coatings, and as solvent.[51,70,71] Advances in the functionalisation of select terpenes within a mixture would forgo the need to purify each terpene from the mixture prior to hydroaminoalkylation. Selective amination would result in the preparation of synthetic terpenoid alkaloids that could be easily separated from unreacted terpene starting materials.

Analysis by GC-MS and NMR spectroscopy of a sample of turpentine[72] from our industry partner, Holmen AB, confirms the presence α-pinene (57 mol%), β-pinene (26 mol%), and limonene (9 mol%) as the most abundant monoterpenes. Although α-pinene constitutes 57% of our sample of turpentine, our attempts at hydroaminoalkylation using a commercially pure sample were not successful (see ESI†). This lack of reactivity is presumably due to the steric hinderance associated with this trisubstituted alkene.[47] If α-pinene is non-reactive with our catalyst, we wondered if it could act as reaction solvent, thereby allowing us to avoid the addition of further solvent, such as toluene. Thus, turpentine would serve as a source of reactive alkenes, β-pinene and limonene, and the remainder would serve as reaction solvent (Scheme 5).

Here, *N*-methylaniline was added to a suspension of 10 mol% $\mathbf{Ta(CH_2SiMe_3)_3Cl_2}$ and $\mathbf{L^-Na^+}$ in turpentine in a 1 : 1 amine : turpentine ratio. The neat reaction mixture was then heated at 145 °C for 24 hours. High vacuum was next applied after the reaction to remove all volatiles, and the resulting crude product mixture was dissolved in toluene-d_8, and filtered over a Celite™-packed Pasteur pipette for ^{1}H NMR yield quantification. A yield of 38% of **3** and 70% of **4** were measured by ^{1}H NMR spectroscopy, respectively. Product formation was confirmed by the appearance of new signals corresponding to the product methyl C–H resonances at 0.99 and 0.72 ppm for **3** and **4**, respectively, after hydrofunctionalisation (Scheme 5). Product formation was further confirmed by GC (see ESI†). Notably, selective reactivity with the geminally substituted alkene of limonene was observed and there was no reactivity with the endocyclic tri-substituted alkene. Finally, purification *via* filtration through a silica gel plug provided a 1.7 : 1 mixture of **3** : **4** in 57% isolated yield relative to the β-pinene and limonene starting material present in the turpentine mixture. This represents a total isolated yield of 20% of aminated material from the initial turpentine mixture. When toluene was added as reaction solvent, **3** and **4** were furnished in 33% and 60% NMR yields, respectively, further demonstrating the efficiency of the neat turpentine reaction (see ESI†). Thus, the hydroaminoalkylation of a turpentine mixture serves to demonstrate the capability our tantalumureate catalyst to react with select terpenes within a complex biomass-sourced alkene mixture containing at least 6 monoterpenes (see ESI† for monoterpene species).

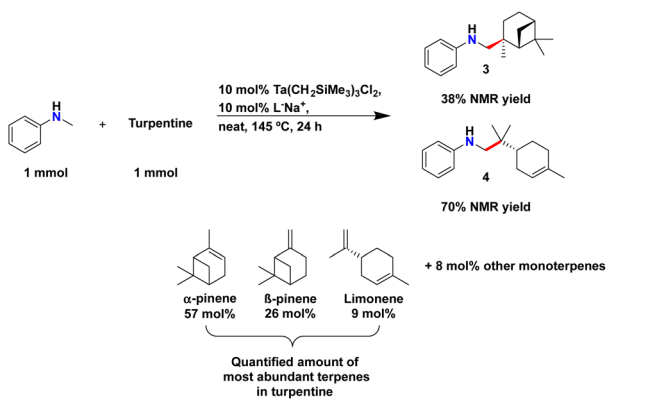

Scheme 5 Synthesis of **3** and **4** in near turpentine. **TMB** was used as internal standard for ^{1}H NMR yields & ratios.

Next, we sought to study the reactivity of our catalyst with structurally complex sesquiterpenes containing multiple alkenes within their frameworks. β-Caryophyllene and its isomer humulene are examples of sesquiterpenes and are notable for providing the 'hoppy' aroma in beer (Fig. 1).[73,74] Both sesquiterpenes contain unique structural features such as trisubstituted alkenes as well as endo- or exocyclic disubstituted alkenes. These different unsaturated Csp^2–Csp^2 bonds create opportunities to explore factors controlling alkene chemoselectivity in hydroaminoalkylation.

We first tested β-caryophyllene for reactivity in the presence of our catalyst and *N*-methylaniline (Scheme 6). β-Caryophyllene contains an exocyclic geminal disubstituted alkene and an *E*-endocyclic trisubstituted alkene within its framework. Based upon reactivity trends with limonene and β-pinene we anticipated selective functionalization of geminal disubstituted alkene of β-caryophyllene.

On NMR tube scale, 1 equivalent of *N*-methylaniline and 1 equivalent of β-caryophyllene were sequentially added to a solution of 10 mol% of $\mathbf{Ta(CH_2SiMe_3)_3Cl_2}$ and $\mathbf{L^-Na^+}$ in toluene-d_8. The reaction mixture was heated to 130 °C for 24 hours.[75] ^{1}H NMR spectroscopy was used to monitor the disappearance of the *ortho* C–H resonances of *N*-methylaniline and a new signal at 6.50 ppm for product formation (Scheme 6). A ^{1}H NMR yield of 76% could be calculated for the new product by using TMB as internal standard. GC-MS analysis of the reaction mixture after heating confirmed that a single monoaminated product was formed.

Remarkably, structural analysis of this product by 2D NMR spectroscopy revealed the selective formation of **5**, which results from selective hydroaminoalkylation of the endocyclic trisubstituted alkene while the geminal disubstituted alkene remained unreacted. Our structural assignment was particularly aided by diagnostic HSQC and HMBC NMR (see ESI† for

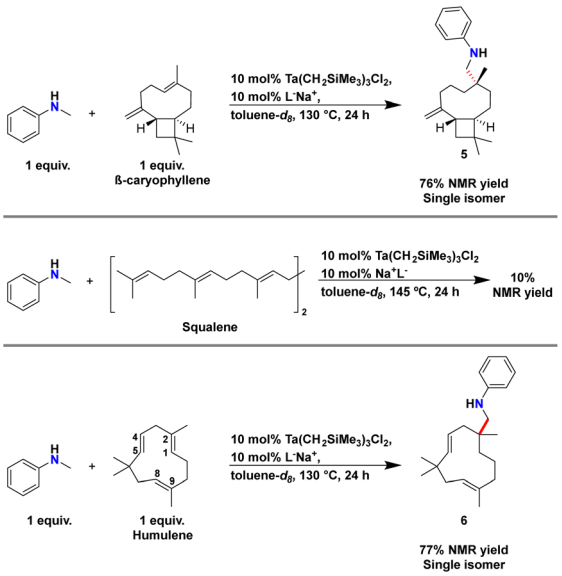

Scheme 6 Synthesis of **5** and **6** by hydroaminoalkylation and attempt at squalene functionalisation. Yields were calculated by ^{1}H NMR spectroscopy using **TMB** as internal standard.

discussion). The relative diastereoselectivity and connectivity were further confirmed by X-ray crystallography by generating an ammonium chloride salt from **5** (see ESI†). This remarkably chemoselective and diastereospecific reactivity at a sterically hindered site represents a dramatic departure from previously reported reactivity trends in hydroaminoalkylation.

Such reactivity with the trisubstituted alkene was completely unexpected. As a result, we questioned the driving force inherent to our terpene substrate that must be at play to unlock such unprecedented reactivity. It is established that *E*-endocyclic alkenes carry considerably more strain energy relative to their *Z*-endocyclic counterparts, therefore we propose 'strain release' within a cyclic framework could be a major driving force in this observed reactivity.[76]

To probe 'strain release' effects with our tantalum catalyst, the reactivity of squalane, a triterpene containing an acyclic series of non-conjugated *E*-trisubstituted alkenes, was tested with *N*-methylaniline (Scheme 6) using comparable reaction conditions. After heating at 145 °C for 24 hours, a ^{1}H NMR yield of 10% was measured, which is consistent with no catalytic turnover. These results suggest that the strain of *E*-trisubstituted endocyclic alkenes provide a crucial driving force for unlocking challenging alkene functionalization. To confirm this hypothesis, we turned our attention next to humulene which also bears 2 *E*-endocyclic trisubstituted alkenes as well as an *E*-endocyclic disubstituted alkene in its framework (Scheme 6).

Similar to the synthesis of **5**, 1 equivalent of each *N*-methylaniline and humulene were added to a solution of 10 mol% of **Ta(CH$_2$SiMe$_3$)$_3$Cl$_2$** and **L$^-$Na$^+$** in toluene-d_8. The reaction mixture was then heated at 130 °C for 24 hours. ^{1}H NMR spectroscopy was used to monitor the appearance of a new set of signals for the *ortho* C–H resonances of the aniline moiety at 6.51 ppm and once again, 2D NMR spectroscopic analysis indicated the formation of **6**, a product from trisubstituted alkene functionalisation. A ^{1}H NMR yield of 77% was determined and GC-MS analysis of the reaction mixture after heating confirmed that a single monoaminated product was produced.

Specifically, trisubstituted alkene **C1–C2** was selectively functionalised according to structural analysis by 2D NMR spectroscopy of **6**. HSQC and HMBC correlations also suggest that **C4–C5** and **C8–C9** remain untransformed (see ESI† for discussion). It is interesting that the *E*-disubstituted alkene remains unreacted, even though we have reported the successful functionalization of similar alkenes with tantalum-ureate catalysts.[40] This remarkable chemoselectivity in hydroaminoalkylation is consistent with substrate strain-release being a critical driving force for controlling hydroaminoalkylation reactivity. However, the exquisite selectivity for **C1–C2** over **C8–C9** in hydroaminoalkylation required further analysis.

To further support the structure for **6**, as assigned by NMR spectroscopy, we next sought to obtain a solid-state molecular structure. An ammonium chloride salt of **6** was generated from the addition of HCl to **6**, an oil, in DCM. After 5 minutes of stirring, high vacuum was applied which furnished a crystalline powder (see ESI†). Next, crystals suitable for X-Ray Diffraction (**XRD**) were grown by Et_2O diffusion into a saturated DCM solution of the hydrochloride salt (**6·HCl**) followed by slow solvent evaporation. The solid-state molecular structure of **6·HCl** shows **C1–C2** alkene functionalisation by hydroaminoalkylation and the hydrochlorination of **C8–C9** (formed upon treatment with HCl) while the disubstituted alkene **C4–C5** remains unfunctionalized. This result provides more evidence of the profound electronic effect of **C1–C2** which dictates complete chemoselective reactivity in hydroaminoalkylation.

The selective formation of **5** and **6** show that strain release is dictating reactivity in hydroaminoalkylation. Such strain factors were previously demonstrated to be critical for high epoxidation reactivity as isocaryophyllene (a β-caryophyllene isomer with a *Z*-endocyclic trisubstituted alkene) was reported to be a magnitude less reactive than β-caryophyllene and humulene under the same reaction conditions.[77] Furthermore, calculations and conformational analyses (bond lengths and angles) *via* X-ray crystal structures of β-caryophyllene, humulene, and their derivatives were used to rationalize the preferred reactivity of the same trisubstituted alkenes in epoxidation.[12,77–81] Previous reports have attributed the selectivity observed with humulene to be due to the nearly perpendicular dihedral angle between the plane of the alkene and its allylic σ_{C-C} bonds, creating a strong hyperconjugative effect that maximizes electron density onto **C1–C2** over **C8–C9**.[80] We suggest that a combination of strain release as well as hyperconjugation within natural substrates work synergistically to overcome steric inhibition to realize selective trisubstituted alkene hydroaminoalkylation.

Previous computational results supporting hydroaminoalkylation reaction outcome analysis have asserted electronic features as being critical for regioselective reactivity of terminal alkenes.[68] Recent results reported for the tantalum-ureate catalyst system used here have shown that substrate electronic effects in substituted styrene derivatives also impact regioselectivity.[31] We attribute the high regioselectivity observed in β-caryophyllene and humulene to the preferred orientation of the least sterically hindered carbon of the alkene α-to tantalum in the formation of the aza-metallacyclopentane intermediate from alkene insertion. Like terminal alkenes, the less substituted carbon is appropriate for the accumulation of greater negative charge, resulting in preferred metallacycle formation with the electrophilic metal centre.[68] Overall, this work has unlocked new strategies in hydroaminoalkylation reactivity through substrate-controlled alkene strain and stereoelectronics effects.

Conclusions

In summary, we report the use of naturally sourced terpenes as an abundant starting-material pool to install nitrogen functionality with high regio- and diastereoselectivity *via* tantalum catalysed hydroaminoalkylation. Naturally sourced 1,3-butadienes produced selectively the (*Z*)-1,4-*addition* product, a new achievement in early-metal catalysed hydroaminoalkylation. As well, we were able to demonstrate the selectivity of our catalyst to achieve select terpene functionalisation in a neat turpentine mixture to produce aminated β-pinene and limonene derivatives. New synthetic reactivity was explored with β-caryophyllene and humulene. These complex substrates revealed that electron rich, strained trisubstituted alkenes can undergo chemoselective functionalisation. We propose that the selectivity is dictated by stereoelectronic and strain release effects to yield unique aminated sesquiterpenoids. Overall, this work featuring terpene substrates has revealed new tools in hydroaminoalkylation for predicting chemoselective, diastereoselective, and regioselective outcomes in diene and alkene hydroaminoalkylation. These insights expand the understanding and substrate scope in the direct catalytic addition of amines to alkenes in a 100% atom economic transformation.

Data availability

The authors confirm that the data supporting the findings of this study are available within the article [and/or] its ESI.†

Author contributions

L. L. S. and H. L. T. directed this project and revised the manuscript. C. H. M. Z conducted all catalytic experiments and syntheses. B. E. N. collected XRD data and solved X-ray structures.

Conflicts of interest

The authors declare the following competing financial interest(s): The Ta catalyst used in this work is patented (PCT/CA2018/050619).

Acknowledgements

We thank Dr M. Ezhova of UBC NMR facility for assistance in characterization of product structures, and B. Herring of UBC Shared Instrument Facility for assisting in monoterpene identification in turpentine by GC.

As well, we thank NSERC, Canada Research Chairs program, UBC Energy Reduction in Mechanical Pulping, and UBC for funding. We also thank Holmen AB for providing a sample of turpentine. B. E. N. and C. H. M. Z thank NSERC for scholarships.

This work was conducted as part of the Energy Reduction in Mechanical Pulping program, funded by a Collaborative Research and Development Grant provided by NSERC (Grant No. CRDPJ 538628-19) and the following partners: AB Enzymes, Alberta Newsprint Company, BC Hydro, BC Institute of Technology, Canfor, Paper Excellence, FPInnovations, Holmen Paper, McMaster University, Millar Western, The University of British Columbia Pulp and Paper Centre, University of Victoria, West Fraser, and Valmet, who we greatly thank for their continuous support.

References

1 R. B. Woodward and W. E. Doering, *J. Am. Chem. Soc.*, 1944, **66**, 849.
2 A. Hinman and J. Du Bois, *J. Am. Chem. Soc.*, 2003, **125**, 11510–11511.
3 W. L. Scott and D. A. Evans, *J. Am. Chem. Soc.*, 1972, **94**, 4779–4780.
4 Z. G. Brill, M. L. Condakes, C. P. Ting and T. J. Maimone, *Chem. Rev.*, 2017, **117**, 11753–11795.
5 R. J. Nyamwihura and I. V. Ogungbe, *RSC Adv.*, 2022, **12**, 11346–11375.
6 D. Cox-Georgian, N. Ramadoss, C. Dona and C. Basu, *Med. Plants From Farm to Pharm*, 2019, pp. 333–359.
7 S. J. Greay and K. A. Hammer, *Phytochem. Rev.*, 2011, **14**, 1–6.
8 M. Zielińska-Błajet and J. Feder-Kubis, *Int. J. Mol. Sci.*, 2020, **21**, 7078.
9 S. R. Ferrarini, C. S. Graebin, J. Limberger, R. F. Canto, D. O. Dias, R. G. da Rosa, M. de F. Madeira and V. L. Eifler-Lima, *Mem. Inst. Oswaldo Cruz*, 2008, **103**, 773–777.
10 S. Liao, S. Shang, M. Shen, X. Rao, H. Si, J. Song and Z. Song, *Bioorg. Med. Chem. Lett.*, 2016, **26**, 1512–1515.
11 W. B. Cunningham, J. D. Tibbetts, M. Hutchby, K. A. Maltby, M. G. Davidson, U. Hintermair, P. Plucinski and S. D. Bull, *Green Chem.*, 2020, **22**, 513–524.

12 C. Lescot, B. Darses, F. Collet, P. Retailleau and P. Dauban, *J. Org. Chem.*, 2012, **77**, 7232–7240.
13 M. C. White and J. Zhao, *J. Am. Chem. Soc.*, 2018, **140**, 13988–14009.
14 Q. Wang, H. Jung, D. Kim and S. Chang, *J. Am. Chem. Soc.*, 2023, **145**, 24940–24951.
15 C. S. Kuai, D. W. Ji, C. Y. Zhao, H. Liu, Y. C. Hu and Q. A. Chen, *Angew. Chem., Int. Ed.*, 2020, **59**, 19115–19120.
16 L. Bareille, S. Becht, J. L. Cui, P. Le Gendre and C. Moïse, *Organometallics*, 2005, **24**, 5802–5806.
17 A. Perrier, V. Comte, C. Moïse and P. Le Gendre, *Chem. – Eur. J.*, 2010, **16**, 64–67.
18 A. Çelik, S. L. Flitsch and N. J. Turner, *Org. Biomol. Chem.*, 2005, **3**, 2930–2934.
19 C. G. Vieira, M. C. De Freitas, K. C. B. De Oliveira, A. De Camargo Faria, E. N. Dos Santos and E. V. Gusevskaya, *Catal. Sci. Technol.*, 2015, **5**, 960–966.
20 T. S. Chamblee, R. R. Weikel, S. A. Nolen, C. L. Liotta and C. A. Eckert, *Green Chem.*, 2004, **6**, 382–386.
21 E. Vitaku, D. T. Smith and J. T. Njardarson, *J. Med. Chem.*, 2014, **57**, 10257–10274.
22 S. D. Roughley and A. M. Jordan, *J. Med. Chem.*, 2011, **54**, 3451–3479.
23 D. G. Brown and J. Boström, *J. Med. Chem.*, 2016, **59**, 4443–4458.
24 J. Li, J. S. Cisar, C. Y. Zhou, B. Vera, H. Williams, A. D. Rodríguez, B. F. Cravatt and D. Romo, *Nat. Chem.*, 2013, **5**, 510–517.
25 B. M. Trost, *Angew. Chem., Int. Ed.*, 1995, **34**, 259–281.
26 R. C. DiPucchio, S.-C. Rosca and L. L. Schafer, *J. Am. Chem. Soc.*, 2022, **144**, 11459–11481.
27 P. M. Edwards and L. L. Schafer, *Chem. Commun.*, 2018, **54**, 12543–12560.
28 M. Manßen and L. L. Schafer, *Trends Chem.*, 2021, **3**, 428–429.
29 S. M. Thullen and T. Rovis, *J. Am. Chem. Soc.*, 2017, **139**, 15504–15508.
30 M. Manßen, D. Deng, C. H. M. Zheng, R. C. DiPucchio, D. Chen and L. L. Schafer, *ACS Catal.*, 2021, **11**, 4550–4560.
31 R. C. DiPucchio, K. E. Lenzen, P. Daneshmand, M. B. Ezhova and L. L. Schafer, *J. Am. Chem. Soc.*, 2021, **143**, 11243–11250.
32 A. E. Nako, J. Oyamada, M. Nishiura and Z. Hou, *Chem. Sci.*, 2016, **7**, 6429–6434.
33 J. Dörfler, T. Preuß, A. Schischko, M. Schmidtmann and S. Doye, *Angew. Chem., Int. Ed.*, 2014, **53**, 7918–7922.
34 T. Kaper, M. Fischer, H. Thye, D. Geik, M. Schmidtmann, R. Beckhaus and S. Doye, *Chem. – Eur. J.*, 2021, **27**, 6899–6903.
35 P. Verma, J. M. Richter, N. Chekshin, J. X. Qiao and J. Q. Yu, *J. Am. Chem. Soc.*, 2020, **142**, 5117–5125.
36 G. Lahm and T. Opatz, *Org. Lett.*, 2014, **16**, 4201–4203.
37 M. Schinkel, L. Wang, K. Bielefeld and L. Ackermann, *Org. Lett.*, 2014, **16**, 1876–1879.
38 D. C. Schmitt, J. Lee, A.-M. R. Dechert-Schmitt, E. Yamaguchi and M. J. Krische, *Chem. Commun.*, 2013, **49**, 6096–6098.
39 E. N. Bahena, S. E. Griffin and L. L. Schafer, *J. Am. Chem. Soc.*, 2020, **142**, 20566–20571.
40 R. C. DiPucchio, S.-C. Roşca and L. L. Schafer, *Angew. Chem., Int. Ed.*, 2018, **57**, 3469–3472.
41 E. Chong, J. W. Brandt and L. L. Schafer, *J. Am. Chem. Soc.*, 2014, **136**, 10898–10901.
42 P. Garcia, Y. Y. Lau, M. R. Perry and L. L. Schafer, *Angew. Chem., Int. Ed.*, 2013, **52**, 9144–9148.
43 P. Eisenberger, R. O. Ayinla, J. M. P. Lauzon and L. L. Schafer, *Angew. Chem., Int. Ed.*, 2009, **48**, 8361–8365.
44 P. Daneshmand, S. C. Roşca, R. Dalhoff, K. Yin, R. C. Dipucchio, R. A. Ivanovich, D. E. Polat, A. M. Beauchemin and L. L. Schafer, *J. Am. Chem. Soc.*, 2020, **142**, 15740–15750.
45 M. Manßen, S. S. Scott, D. Deng, C. H. M. Zheng and L. L. Schafer, *Green Chem.*, 2023, **25**, 2629–2639.
46 E. Nuñez Bahena, S. A. Sirohey and L. L. Schafer, *Organometallics*, 2023, **42**, 1291–1299.
47 R. C. DiPucchio, S. Rosca, G. Athavan and L. L. Schafer, *ChemCatChem*, 2019, **11**, 3871–3876.
48 S. S. Scott, S. C. Roşca, D. J. Gilmour, P. Brant and L. L. Schafer, *ACS Macro Lett.*, 2021, **10**, 1266–1272.
49 S. S. Scott, B. Kaur, C. H. M. Zheng, P. Brant, D. J. Gilmour and L. L. Schafer, *J. Am. Chem. Soc.*, 2023, **145**, 22871–22877.
50 C. H. M. Zheng, D. A. Balatsky, R. C. Dipucchio and L. L. Schafer, *Org. Lett.*, 2022, **24**, 6571–6575.
51 M. Golets, S. Ajaikumar and J. P. Mikkola, *Chem. Rev.*, 2015, **115**, 3141–3169.
52 A. Perrier, M. Ferreira, J. N. H. Reek and J. I. Van Der Vlugt, *Catal. Sci. Technol.*, 2013, **3**, 1375–1379.
53 H. C. Brown and N. N. Joshi, *J. Org. Chem.*, 1988, **53**, 4059–4062.
54 F. Xianjie, P. Yu and B. Morandi, *Science*, 2016, **351**, 832–836.
55 E. V. Gusevskaya, J. Jiménez-Pinto and A. Börner, *ChemCatChem*, 2014, **6**, 382–411.
56 J. Zhang, C. G. Yang and C. He, *J. Am. Chem. Soc.*, 2006, **128**, 1798–1799.
57 J. V. Obligacion and P. J. Chirik, *J. Am. Chem. Soc.*, 2013, **135**, 19107–19110.
58 P. Anastas and N. Eghbali, *Chem. Soc. Rev.*, 2010, **39**, 301–312.
59 M. Lewandowski, M. Jaoui, J. H. Offenberg, J. D. Krug and T. E. Kleindienst, *Atmos. Chem. Phys.*, 2015, **15**, 3773–3783.
60 E. Nuñez Bahena, K. Hosseini, S. Galván Curto and L. L. Schafer, *Chem. Sci.*, 2024, DOI: **10.1039/D4SC00636D**.
61 T. Preuß, W. Saak and S. Doye, *Chem. – Eur. J.*, 2013, **19**, 3833–3837.
62 J. Dörfler, T. Preuß, C. Brahms, D. Scheuer and S. Doye, *Dalton Trans.*, 2015, **44**, 12149–12168.
63 J. M. Lauzon, P. Eisenberger, S.-C. Roşca and L. L. Schafer, *ACS Catal.*, 2017, **7**, 5921–5931.
64 M. Manßen, N. Lauterbach, J. Dörfler, M. Schmidtmann, W. Saak, S. Doye and R. Beckhaus, *Angew. Chemie Int. Ed.*, 2015, **54**, 4383–4387.
65 A. L. Reznichenko and K. C. Hultzsch, *J. Am. Chem. Soc.*, 2012, **134**, 3300–3311.

66 G. Luo, F. Liu, Y. Luo, G. Zhou, X. Kang, Z. Hou and L. Luo, *Organometallics*, 2019, **38**, 1887–1896.
67 N. Thoben, T. Kaper, S. de Graaff, L. Gerhards, M. Schmidtmann, T. Klüner, R. Beckhaus and S. Doye, *ChemPhysChem*, 2023, **24**, e202300370.
68 F. Liu, G. Luo, Z. Hou and Y. Luo, *Organometallics*, 2017, **36**, 1557–1565.
69 D. J. Gilmour, J. M. P. Lauzon, E. Clot and L. L. Schafer, *Organometallics*, 2018, **37**, 4387–4394.
70 Z. Schelz, J. Molnar and J. Hohmann, *Fitoterapia*, 2006, **77**, 279–285.
71 B. Mercier, J. Prost and M. Prost, *Int. J. Occup. Med. Environ. Health*, 2009, vol. 22, pp. 331–342.
72 Our sample of turpentine was extracted via steam recovery.
73 S. T. Katsiotis, C. R. Langezaal and J. J. C. Scheffer, *Planta Med.*, 1989, **55**, 634–634.
74 F. Francomano, A. Caruso, A. Barbarossa, A. Fazio, C. La Torre, J. Ceramella, R. Mallamaci, C. Saturnino, D. Iacopetta and M. S. Sinicropi, *Appl. Sci.*, 2019, **9**, 5420.
75 Increasing reaction temperature results in lower product yields.
76 K. J. Shea and J. S. Kim, *J. Am. Chem. Soc.*, 1992, **114**, 3044–3051.
77 B. Steenackers, A. Neirinckx, L. De Cooman, I. Hermans and D. De Vos, *ChemPhysChem*, 2014, **15**, 966–973.
78 P. J. Li, G. Dräger and A. Kirschning, *Org. Lett.*, 2019, **21**, 998–1001.
79 E. Grau and S. Mecking, *Green Chem.*, 2013, **15**, 1112–1115.
80 U. Neuenschwander, B. Czarniecki and I. Hermans, *J. Org. Chem.*, 2012, **77**, 2865–2869.
81 S. Wang, Y. Li, H. Zhou, L. Wang and R. Wang, *J. Org. Chem.*, 2022, **87**, 8648–8655.